On the Adequacy of Chemiluminescence as a Measure for Heat Release in Turbulent Flames With Mixture Gradients

Martin Lauer
e-mail: lauer@td.mw.tum.de

Thomas Sattelmayer

Lehrstuhl für Thermodynamik,
Technische Universität München,
Boltzmannstraße 15,
85748 Garching, Germany

The determination of the heat release in technical flames is commonly done via bandpass filtered chemiluminescence measurements in the wavelength range of OH^* or CH^* radicals, which are supposed to be a measure for the heat release rate. However, these indirect heat release measurements are problematic because the measured intensities are the superposition of the desired radical emissions and contributions from the broadband emissions of CO_2^*. Furthermore, the chemiluminescence intensities are strongly affected by the local air excess ratio of the flame and the turbulence intensity in the reaction zone. To investigate the influence of these effects on the applicability of chemiluminescence as a measure for the heat release rate in turbulent flames with mixture gradients, a reference method is used, which is based on the first law of thermodynamics. It is shown that although the integral heat release can be correlated with the integral chemiluminescence intensities, the heat release distribution is not properly represented by any signal from OH^* or CH^*. No reliable information about the spatially resolved heat release can be obtained from chemiluminescence measurements in flames with mixture gradients.
[DOI: 10.1115/1.4000126]

1 Introduction

The heat release distribution of the flame is the most important parameter for the understanding and prediction of unstable combustion states, such as thermoacoustic instabilities [1–3], pulsed combustion, and flame propagation due to combustion induced vortex breakdown [4]. Also in other research fields such as combustion noise the knowledge of the heat release rate distribution is very important [5–8].

1.1 Basics. The direct measurement of the spatially resolved heat release rate of flames is difficult because existing time resolved and spatially resolved measurement techniques are too complex to be applied to the above mentioned research fields [9]. As a consequence, traditionally the light emission of the flame, the so-called chemiluminescence, is used as an indirect measure for the heat release rate. The chemiluminescence spectrum of a hydrocarbon flame consists of the emissions from the radicals OH^*, CH^*, and C_2^*, and of CO_2^* emissions. The radicals emit light in narrow spectral bands. These emissions are superimposed by the broadband emissions from CO_2^*, as shown in Fig. 1. In most studies narrow bandpass filters in the wavelength range of OH^*, CH^*, or C_2^* are used because these radicals are supposed to correlate with the heat release rate.

For laminar premixed flames the applicability of chemiluminescence as an indirect measure for heat release has been shown in many experimental and theoretical studies. Most authors consistently report a linear increase in the integral chemiluminescence intensity with increasing fuel-flow rate, and a decreasing intensity with increasing air excess ratio [10–14]. But for turbulent flames the correlation between chemiluminescence and heat release is more complicated and not fully understood, yet. A positive monotonic dependency of the chemiluminescence intensity on fuel-flow rate has been reported, similar to laminar flames [10,13,15], as well as contrary observations have been made [11,12,16].

1.2 Motivation. For confined and adiabatic turbulent flames the integral chemiluminescence intensity has successfully been used to monitor the integral heat release of the flame in many studies (e.g., Refs. [1,3,17]). The correlation between heat release and chemiluminescence has been determined empirically in these studies. This led to the unconfirmed conclusion that also the spatially resolved heat release can be obtained via chemiluminescence, and that the chemiluminescence distribution of a flame can be used as a measure for flame length. This conclusion is questionable because flame parameters such as turbulence intensity, strain rate, and curvature, which influence the chemiluminescence intensity strongly [12,15,16,18], may vary substantially in turbulent flames. Additionally, in applications such as aircraft engines or gas turbines, cooling air enters the flame and dilutes the mixture. This causes mixture gradients, which also influence chemiluminescence intensities.

Another basic problem when measuring chemiluminescence is the use of bandpass filters. The measured signals are the superposition of the desired radical intensities and contributions from the broadband emission of CO_2^*. In turbulent flames the signal from CO_2^* contributions can be of the same order as the radical chemiluminescence or even exceed the radical intensity (Fig. 1).

In this study, the applicability of indirect, spatially resolved heat release measurements via chemiluminescence in turbulent swirl flames is investigated. The effect of mixture gradients and the effect of CO_2^* contributions in bandpass filtered signals are investigated. Additionally the influence of turbulence intensity on the chemiluminescent emissions is shown. The heat release distribution, measured with a reliable reference method, is compared with the distributions obtained from bandpass filtered and CO_2^*

Contributed by the International Gas Turbine Institute (IGTI) of ASME for publication in the JOURNAL OF ENGINEERING FOR GAS TURBINES AND POWER. Manuscript received April 9, 2009; final manuscript revised April 14, 2009; published online March 18, 2010. Editor: Dilip R. Ballal.

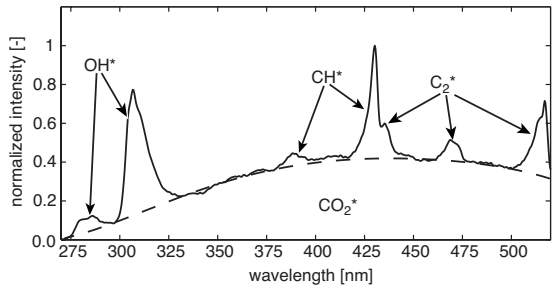

Fig. 1 Chemiluminescence spectrum of a stoichiometric premixed methane-air flame. The narrowband radical emissions from OH^*, CH^*, and C_2^* are superimposed by the broadband emission from CO_2^*.

contribution corrected chemiluminescence measurements.

In Sec. 2, a short literature review of heat release measurements via chemiluminescence is given and the experimental setup and the flame under investigation are described. Then the reference technique for the calculation of the spatially resolved heat release is briefly described and discussed. After that the measurement techniques used in this study are presented, and the procedure to obtain the radical intensities from bandpass filtered measurements is explained. Finally, the comparison of the heat release determined from chemiluminescence and the reference method is presented.

2 Literature Review

The first experimental investigations on the correlation of chemiluminescent light emissions with the integral heat release of a flame date back to the 1950s. Clark and Bittker [10] investigated the integral chemiluminescence of laminar and weakly turbulent propane-air flames. They found a linear dependency of the chemiluminescence intensity on fuel-flow rate at constant air excess ratios, and a decrease in the intensity with increasing air excess ratio for Reynolds numbers up to 6000.

John and Summerfield [11] investigated the light emissions from CO_2^*, C_2^*, and CH^* in laminar and turbulent flames with Reynolds numbers up to 100,000. For all investigated chemiluminescent species the turbulence was found to reduce the specific intensity of the chemiluminescence. The intensity reduction was found to be stronger for CO_2^* than for C_2^* or CH^*.

Hurle et al. [12] investigated the emissions from C_2^* and CH^* in laminar and moderately turbulent ethylene-air flames. For Reynolds numbers up to 10,000 a linear dependency of chemiluminescence intensity on fuel-flow rate and heat release rate, respectively, has been observed. The slope of the correlation has been found to be a function of the air excess ratio. For Reynolds numbers in the range from 10,000 to 13,000 lower intensities have been observed than expected from linear extrapolation from lower Reynolds numbers. For Reynolds numbers higher than 17,000 decreasing intensities with increasing fuel-flow rate have been observed.

In 1995 Samaniego et al. [13] studied the emissions from CO_2^* in laminar and turbulent premixed methane-air and propane-air flames numerically. They found CO_2^* chemiluminescence to be a good indicator for fuel consumption in flames with varying dilution, strain rate, and air excess ratio. However, in the investigation of Najm et al. [16] a complicated dependency of CO_2^* chemiluminescence on curvature and flow history is reported, which leads to an ambiguous correlation of the chemiluminescence with burning rate and heat release. Furthermore, Najm et al. [16] showed a detailed analysis of the reaction mechanism of the methane oxidation. The relative amounts of carbon in the different possible reaction paths have been quantified. In this analysis Najm et al. [16] concluded that only a small portion of the carbon follows side reaction paths, which lead to the chemiluminescent radicals OH^*, CH^*, and C_2^*. Most of the carbon follows the main reaction path, which may yield some CO_2^* (Fig. 2).

Moreover, it was shown that for stoichiometric to lean flames there is the tendency to transfer carbon from side paths to the main reaction path, which reduces the chemiluminescence intensity from the radicals. Finally Najm et al. [16] concluded that OH^*, CH^*, and C_2^* are not reliable markers for the turbulent flame front, burning rate, or heat release rate because their appearance in the flame is not an indicator for the pathway of carbon oxidation for the main portion of carbon.

Lee and Santavicca [15] investigated the integral visible chemiluminescent emission from a turbulent swirled flame. They reported a linear dependency of the chemiluminescence signal on fuel-flow rate and an exponentially decreasing signal with increas-

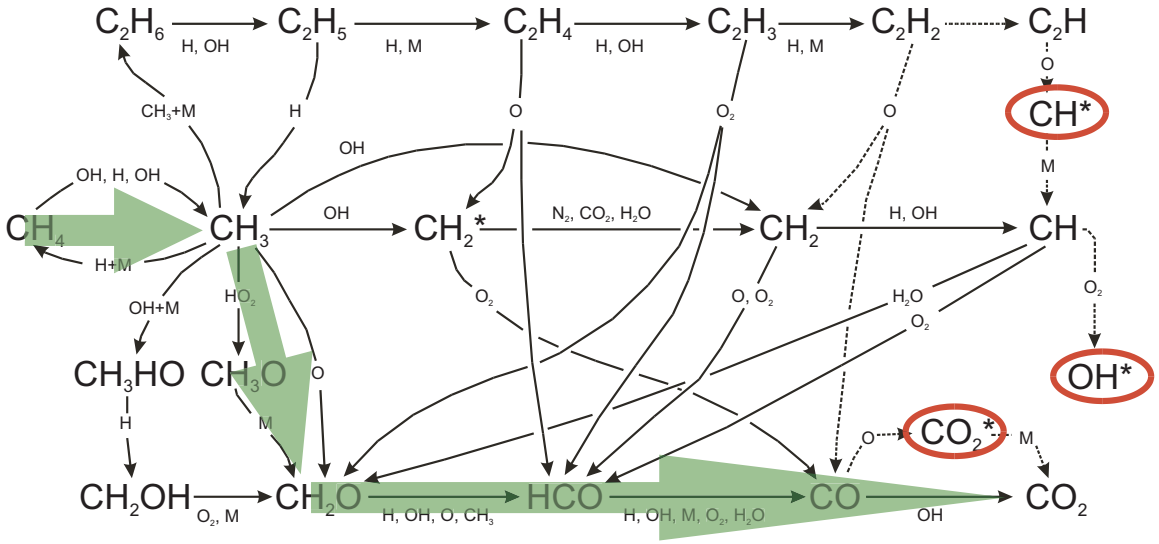

Fig. 2 The simplified methane oxidation mechanism [16]. The main portion of the carbon follows the marked reaction path. Only a small portion follows the side paths, which yield OH^*, CH^*, and C_2^*. From this, Najm et al. [16] concluded that OH^*, CH^*, and C_2^* are not reliable markers for reaction rate or heat release rate in the flame.

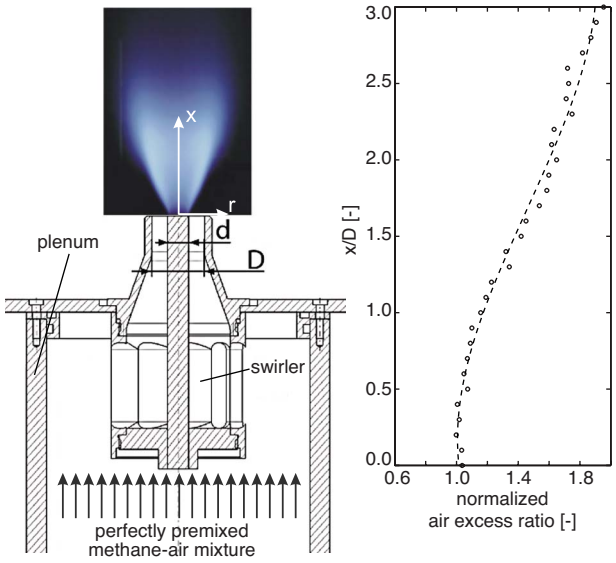

Fig. 3 Sketch of the test rig and exemplary axial air excess ratio distribution due to ambient air entrainment

ing air excess ratio. Moreover, they reported a strong influence of premix level, curvature, and stretch on the chemiluminescence signal.

Ayoola et al. [18] used heat release rate imaging to characterize OH^* chemiluminescence as a measure for the spatially resolved heat release rate. Heat release rate imaging is the pixel-by-pixel product of OH and CH_2O planar laser induced fluorescence (PLIF) signals, which correlates very well with the local heat release rate. Several turbulent, premixed, ethylene-fueled flames with Reynolds numbers in the range of 19,000–29,000 were under investigation. OH^* was found to be very sensitive to strain and turbulence. It was observed that strong OH^* chemiluminescence signals emerged from regions within the flame with a relatively low heat release rate. It was also observed that in bluff-body stabilized flames the air excess ratio dependency of the OH^* chemiluminescence was different for different positions in the flame brush. Ayoola et al. [18] concluded that OH^* chemiluminescence is not a reliable indicator for heat release.

In summary, the studies, especially of Hurle et al. [12], Najm et al. [16], Lee and Santavicca [15], and Ayoola et al. [18], showed the problems of heat release measurements via chemiluminescence in turbulent flames. The chemiluminescence signal of all emitting species are strongly affected by turbulence intensity, strain rate, curvature, fuel-flow rate, degree of premixing, and air excess ratio. But these quantities are not necessarily spatially or temporally constant in turbulent flames. Nevertheless, the integral chemiluminescence intensity is often used successfully as a measure for the integral heat release in turbulent flames. This can be explained with the fact that the change in a chemiluminescence relevant quantity, e.g., fuel-flow rate, influences the chemiluminescent emissions in all parts of the flame volume. Thus, a monotonic dependency of the integral light emission and the integral heat release is found and can be evaluated with an empirically determined calibration. This led to the conclusion that also the local heat release can be measured by the local chemiluminescence intensity. The limits of applicability of this conclusion are the main subject of this study.

3 Experimental Setup

The experimental study is carried out with a modular, swirl stabilized burner with center body. The swirl number was held constant at 0.55 in this study. The inner diameter of the nozzle is $D=40$ mm, the diameter of the center body is $d=16$ mm (Fig. 3). Fuel is natural gas with a methane content of 98%. The air-fuel mixture is externally premixed to avoid any mixture fraction fluctuations in plenum and burner. The thermal power can be adjusted in the range from 10 kW to 120 kW, the air excess ratio λ inside the plenum can be varied between 0.8 and 2.0. The test rig is operated with a nonpreheated air-fuel mixture in this study.

3.1 Ambient Air Entrainment. Since the flame is operated unconfined without a combustion chamber, the air excess ratio of the flame is not constant. As Wäsle et al. [19] showed, a linear increase in the axial mass flow downstream of the burner exit occurs due to turbulent mixing in the shear layer between the swirled flow and the quiescent ambient air. As a consequence, the mixture becomes leaner with increasing axial distance from the burner nozzle (Fig. 3, right hand side) [6,20]. This property of unconfined flames was used in the study to explore the influence of radial fuel concentration profiles in partially premixed burners or to mimic air admixing into turbulent confined gas turbine flames leading to mixture gradients, respectively.

3.2 Operating Points. The fuel-flow rate is equivalent to 60 kW of thermal power for all experiments in this study. Eight operating points with air excess ratios ranging from slightly rich mixtures ($\lambda=0.9$) to lean mixtures ($\lambda=1.6$) close to the lean blow-off limit of the burner are investigated. The Reynolds number in the burner nozzle ranges from 25,600 ($\lambda=0.9$) to 43,600 ($\lambda=1.6$).

4 Reference Technique

In this section a brief review of the reference technique is given. This technique is based on the first law of thermodynamics and, thus, is capable to provide the spatially resolved heat release rate of the flame with high accuracy and reliability. The detailed description of the reference technique can be found in Ref. [21]. Because the results derived from the reference technique are very important for the later comparison with chemiluminescence measurements the obtained heat release rate distributions are explicitly discussed for plausibility.

4.1 Basic Approach. The type of flame under investigation in this study can be described as an open, stationary system with constant pressure and chemical reaction. The following equation is derived from the first law of thermodynamics:

$$\dot{q}_{\text{net}} = \rho(\lambda, c) \cdot c_p(\lambda, c) \cdot (\vec{v} \circ \nabla T(\lambda, c)) \tag{1}$$

This equation balances the volumetric net heat release of the flame with the increasing sensible enthalpy due to the combustion. It is valid for flames with equal temperatures of the mixture and the entrained air, e.g., the case without preheat of the air-fuel mixture.

The volumetric net heat release rate of the flame $\dot{q}_{\text{net}}$ is a function of the density ρ of the fluid, the isobaric heat capacity c_p, the fluid velocity $\vec{v}$, and the temperature gradient ∇T. Density, heat capacity, and temperature are functions of the fluid composition, which can be described by the local air excess ratio of the mixture λ and progress variable of combustion c.

In this study all measured experimental variables are time averaged. This gives the time averaged heat release rate of the flame.

4.2 Required Input Parameters. The desired measures for the calculation of the heat release rate from Eq. (1) are the flow velocity $\vec{v}$, the progress variable of combustion c, and the air excess ratio λ. The underlying measurement techniques are described in detail in Sec. 5.

- The flow velocity of the reacting flow is measured via particle image velocimetry (PIV).
- The progress variable of combustion is calculated from OH-PLIF.
- The air excess ratio is measured via the OH^*/CH^* chemilu-

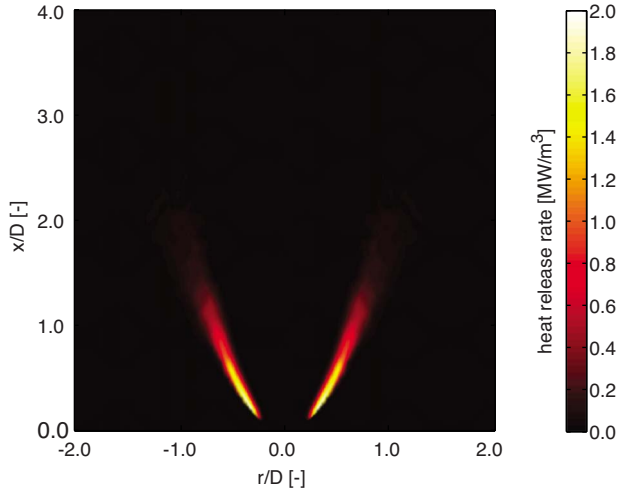

Fig. 4 Heat release rate in the flame midplane of the λ=1.2 operation point

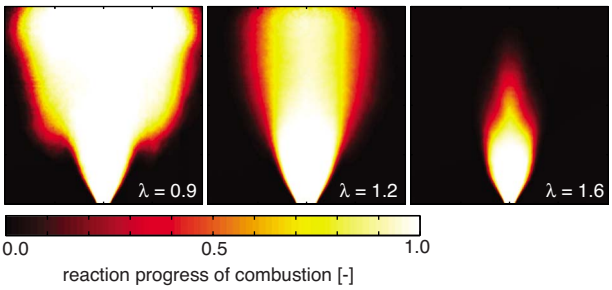

Fig. 6 Time averaged reaction progress of combustion for burner air excess ratios of 0.9, 1.2, and 1.6. With increasing burner air excess ratio an increasing portion of the mixture in the shear layer between the swirled flow and the ambient air is not burnt.

minescence ratio. Despite the shortcomings in determining the heat release rate from the chemiluminescence of a single radical, pointed out in the literature review, it has been shown in a number of studies that the OH^*/CH^* chemiluminescence ratio unambiguously characterizes the air excess ratio of laminar and turbulent flames [20–25].

All measures are taken in the midplane of the flame, which is regarded as the reference plane for the time averaged flame.

4.3 Plausibility Discussion. The result of the determined heat release rate in the flame midplane for the λ=1.2 operating point is shown in Fig. 4.

To check the results of the reference technique, the determined integral heat release of the flames is compared with the heat release expected for the measured fuel-flow rate (Fig. 5). The integral heat release of the λ=0.9 operation point matches the expected value of 60 kW. However, with increasing air excess ratio a linearly decreasing integral heat release can be observed.

This observation can be explained with the ambient air entrainment in the flame. As previous studies have shown, the dilution of the mixture starts about 0.5*D* downstream of the burner nozzle. From there the air excess ratio increases linearly about 0.3 per burner diameter [20,21]. As a consequence, the ignition condition of the mixture degrades increasingly with increasing distance from the burner exit. In the shear layer between the swirled flow and the ambient air an increasing amount of mixture is not burned because of the intense dilution with ambient air. This effect has also been shown by Hoffmann [26] by measuring the composition of the products of turbulent, swirl stabilized, unconfined flames.

The quenching of combustion in the shear layers can also be seen in the spatial distribution of the time averaged reaction progress of combustion (Fig. 6). Close to the burner exit the flame is not influenced by the air entrainment. Further downstream the reaction is increasingly quenched in the shear layers with increasing burner air excess ratio. This can be seen in the smaller flame surface of the leaner flames.

Figure 7 shows the axial heat release distributions of the eight investigated operation points. In this figure three different regimes can be observed.

- For the rich flame (λ=0.9) the heat release distribution is shifted downstream compared with the stoichiometric and lean flames. Because of the rich mixture, additional air has to be transported into the flame to reach favorable ignition conditions. This results in a lower heat release near the burner exit [26].
- For λ=1.0–1.4 the flames show an identical heat release rate up to an axial distance of 0.5*D* downstream of the burner nozzle. Further downstream the heat release distribution is lower for higher air excess ratios due to the increased portion of the fuel flow that is not burned in the leaner flames.
- The λ=1.5–1.6 flames, which are close to the lean blow-off limit of the burner, show lower heat release rates near the burner exit. This might be an indicator for these flames that are not being properly stabilized anymore.

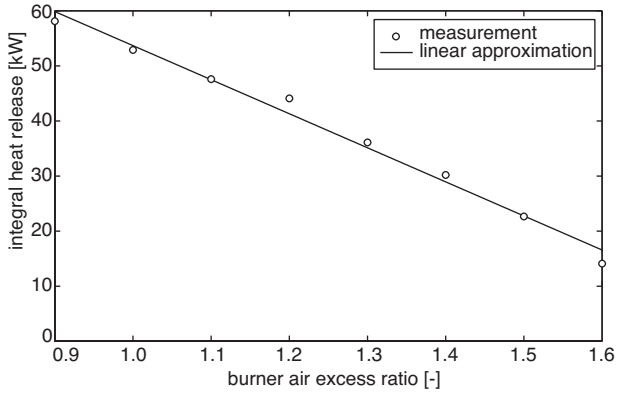

Fig. 5 Integral heat release of the flame determined with the reference technique

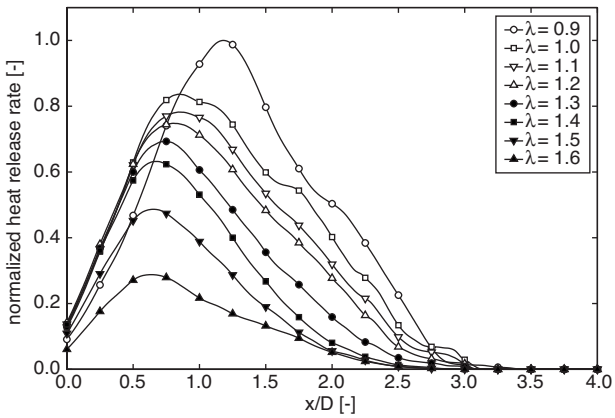

Fig. 7 Axial heat release distribution determined with the reference technique

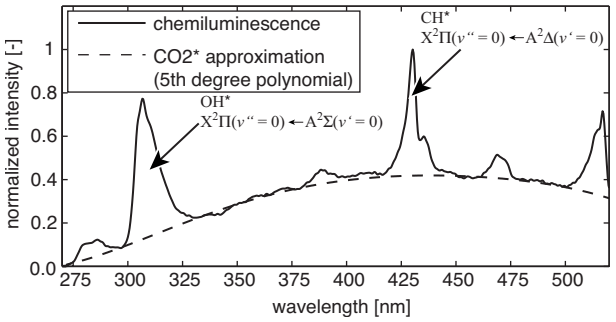

Fig. 8 Chemiluminescence spectrum with the fifth-degree polynomial fit for the CO_2^* emission

Especially the determined heat release rates close to the burner exit for the properly stabilized $\lambda = 1.0-1.4$ flames are in very good agreement with theoretical expectations: The heat release rate is proportional to the volumetric fuel mass flow, which has been kept constant and, therefore, is no function of the burner air excess ratio for the flames under investigation in this study. The determination of identical heat release rates for axial distances up to $0.5D$, which is the region of steepest gradients in the flame volume, shows the potential of the reference technique.

It can be concluded that the results from the reference technique are reasonable and in good agreement with theoretical expectations and former studies.

5 Measurement Techniques and Data Processing

The strongest chemiluminescent emissions emerge from the $X^2\Pi_i(v''=0) \leftarrow A^2\Sigma^+(v'=0)$ transition of OH^* around 306.4 nm and from the $X^2\Pi(v''=0) \leftarrow A^2\Delta(v'=0)$ transition of CH^* around 431.5 nm (Fig. 8). The chemiluminescence from these two transitions is under investigation in this study and is compared with the heat release rate obtained with the reference technique. C_2^* is not considered because C_2^* can only be seen in rich to slightly lean flames. For air excess ratios larger than 1.3 the C_2^* intensity is close to zero.

5.1 Bandpass Filtered Chemiluminescence. The bandpass filtered chemiluminescence signals are detected with a high speed camera with a fiber optically coupled image intensifier and a silica glass camera lens. The lens has a focal length of 45 mm and a maximum aperture of 1:1.8. The spatial resolution of the CMOS (complementary metal oxide semiconductor) sensor of the camera is 1024×1024 pixels. For each measurement 2048 images are captured and averaged. The averaged images are deconvoluted to obtain the spatially resolved chemiluminescence intensities in the flame midplane [27]. Three bandpass filters are used in this study.

- The chemiluminescence of the OH^* transition with superimposed CO_2^* background is measured with an interference filter with a maximum transmission of 16.57% at 309.65 nm and a half-power bandwidth of 5.1 nm.
- The chemiluminescence of the CH^* transition with superimposed CO_2^* background is measured with an interference filter with a maximum transmission of 48.63% at 431.39 nm and a half-power bandwidth of 5.3 nm
- A third interference filter with a maximum transmission of 68.18% at 456.42 nm and a half-power bandwidth of 1.2 nm is used. The measurement signal from this filter gives a characteristic value for the CO_2^* chemiluminescence, which is used to obtain the CO_2^* contribution corrected integral values of the radical transitions from the bandpass filtered OH^* and CH^* signals (see Sec. 5.5).

5.2 Spectrally Resolved Chemiluminescence. The used spectrometer is an Acton Research Corporation SpectraPro-275. The attached camera is identical to the camera used for the bandpass filtered measurements. The optical system of the spectrometer is a Czerny-Turner type with an inline optical path. The focal length is 275 mm with an aperture ratio of 1:3.8. The used grating in this study has 150 g/mm, allowing the observation of approximately 300 nm of the flame spectrum with the attached camera. The slit width of the spectrometer is set to 10 μm in this study. 2048 spectra are averaged for each operation point.

5.3 Velocity and Turbulence Intensity. The mean velocity field for the reference technique and the spatially resolved turbulence intensity, respectively, are measured via PIV. A high speed double cavity Nd:YLF (neodymium-doped yttrium lithium fluoride) laser (527 nm, 10 mJ/pulse) is used. The light sheet has a height of four burner exit diameters. The width is about 2 mm. In this study the double pulses are separated by 20 μs. The detection camera is a high speed CMOS camera with a 1024×1024 pixel sensor. The camera uses an 85 mm focal length lens with a maximum aperture of 1:1.4. However, the aperture was closed to 1:5.6 during the experiments to increase the depth of focus. Additionally, a 532 nm bandpass filter was used for the suppression of disturbing signals from the flame. The maximum transmission of the filter is 90%, the half-power bandwidth 10 nm. TiO_2 particles are used as tracer, due to their high temperature resistance.

The double frames were analyzed with a commercial software. The interrogation area measured 16×16 pixels. A three-step adaptive cross-correlation with 8 pixel separation was used. For each operation point 1024 image pairs are recorded and evaluated. From these data the time averaged velocity field of the flame and the spatially resolved turbulence intensity are calculated.

5.4 Reaction Zone. To characterize the reaction zone of the flame OH-PLIF measurements are used. From the sudden increase in the hydroxyl radical concentration, the boundary between the burned gas and the unburned gases can be detected [28]. A Rhodamine 6 G operated, frequency doubled dye laser, pumped with a Nd:YAG (neodymium-doped yttrium aluminum garnet) laser, is used for excitation of the $Q_1(6)$ line in the $A^2\Sigma^+(v'=1) \leftarrow X^2\Pi(v''=0)$ transition of the hydroxyl radical at 282.925 nm. The resulting fluorescence signal of the excited radicals is frequency shifted due to collisional energy transfer processes. The laser system is operated with 1 kHz repetition rate and 80 μJ pulse energy. The illuminated height of the flame is four burner exit diameters. The fluorescence signal around 306.4 nm is bandpass filtered for the suppression of scattered laser light. The detection camera and lens are identical to the bandpass filtered measurements.

5.5 Subtraction of the CO_2^* Contribution. In spectrally resolved chemiluminescence measurements the broadband emission from CO_2^* can be identified easily and the desired emissions from the radicals can be isolated. This is not possible in a single bandpass filtered measurement. However, spectrometer measurements only provide one-dimensional spatial resolution, whereas bandpass filtered measurements provide a two-dimensional spatial resolution.

A new measurement and data processing procedure is used to separate radical and CO_2^* chemiluminescence in bandpass filtered measurements. In the first step of this procedure chemiluminescence spectra of all operating points have been measured. From this data it was found that the broadband CO_2^* signal can be approximated with a polynomial of fifth degree with high accuracy (Fig. 8). The polynomial fit has been found to be self-similar for all investigated operating points. Moreover, it has been found that the shape of the $X^2\Pi_i(v''=0) \leftarrow A^2\Sigma^+(v'=0)$ transition of OH^* and of the $X^2\Pi(v''=0) \leftarrow A^2\Delta(v'=0)$ transition of CH^* are self-similar, too. However, the shapes of the radical transitions are too complex to be approximated by polynomial fits. Thus, they are defined

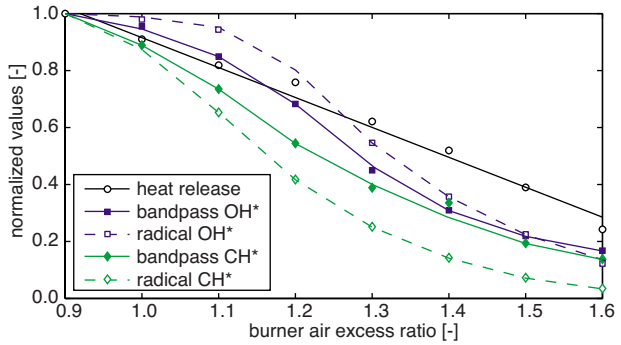

Fig. 9 Comparison of the integral chemiluminescence intensities and the heat release of the flame. All variables are normalized to their maximum value.

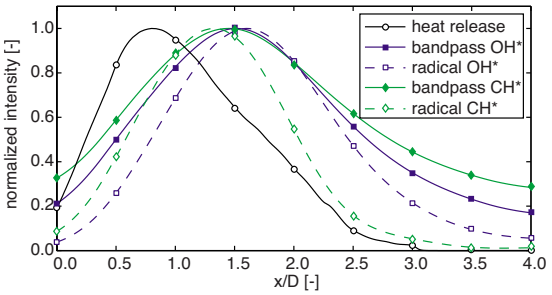

Fig. 10 Comparison of the axial chemiluminescence distribution of bandpass filtered and CO_2^* contributions corrected OH^* and CH^* with the axial heat release distribution

pointwise. The chemiluminescence of CO_2^* and the radicals, respectively, can be written as the product of the self-similar function and a specific proportionality constant.

With this information the bandpass filtered chemiluminescence signal in the wavelength range of OH^* can be approximated mathematically

$$S_{\mathrm{BP,310\ nm}} = \int_0^\infty ((C_{\mathrm{OH}^*} \cdot F_{\mathrm{OH}^*}(\lambda_\nu) + C_{\mathrm{CO}_2^*} \cdot F_{\mathrm{CO}_2^*}(\lambda_\nu)) \cdot T_{\nu,\mathrm{OH}^*}(\lambda_\nu))d\lambda_\nu \quad (2)$$

In this equation S_{BP} denotes the bandpass filtered measurement signal, F denotes the self-similar descriptions of the radical and CO_2^* chemiluminescence, C denotes the corresponding proportionality constants, and T_ν denotes the wavelength dependent transmission of the used bandpass filter. λ_ν is the wavelength.

The self-similar descriptions $F(\lambda_\nu)$ are known from the spectrometer measurements described above, the filter transmission $T(\lambda_\nu)$ is known from the manufacturer. The proportionality constants have to be calculated. $C_{\mathrm{CO}_2^*}$ can be derived from a bandpass filtered measurement in a wavelength range where only CO_2^* is emitting light. Such a wavelength range can be found between the $a^3\Pi_h(v'=0) \leftarrow d^3\Pi_g(v''=2)$ and the $a^3\Pi_h(v'=2) \leftarrow d^3\Pi_g(v''=3)$ transitions of C_2^* at 438 nm and 476 nm, respectively. For this purpose the third bandpass filter described above, centered at 456 nm, is used. Here the measurement signal can be written as follows:

$$S_{\mathrm{BP,456\ nm}} = \int_0^\infty ((C_{\mathrm{CO}_2^*} \cdot F_{\mathrm{CO}_2^*}(\lambda_\nu)) \cdot T_{\nu,\mathrm{CO}_2^*}(\lambda_\nu))d\lambda_\nu \quad (3)$$

The proportionality constant $C_{\mathrm{CO}_2^*}$ can be obtained by solving Eq. (3) numerically. The proportionality constant C_{OH^*} can then be calculated from Eq. (2). The desired intensity of the radical chemiluminescence is

$$I_{\mathrm{OH}^*} = \int_0^\infty (C_{\mathrm{OH}^*} \cdot F_{\mathrm{OH}^*}(\lambda_\nu))d\lambda_\nu \quad (4)$$

The integral intensity of the CH^* transition can be calculated accordingly.

6 Results and Discussion

Below, the comparison between chemiluminescence and heat release rate from the reference technique is presented for traditionally bandpass filtered chemiluminescence data and for the CO_2^* contribution corrected chemiluminescence intensities from the radical transitions.

6.1 Integral Values. In Fig. 9 the normalized integral values of heat release and chemiluminescence intensities are shown.

It can be seen that all investigated chemiluminescence signals are monotonically decreasing with increasing burner air excess ratio. But all chemiluminescence signals show a more complicate characteristic than the linearly decreasing heat release of the flame. This can be explained with the fact that for the flames investigated in this study a change in the burner air excess ratio also changes the integral heat release of the flame. Thus, the effect from the change in air excess ratio and the effect from the simultaneously changing integral heat release interfere with each other. As a consequence, no direct proportionality between any chemiluminescence signal and the heat release can be observed. It can also be seen that for the comparison of the integral heat release and the integral chemiluminescence intensities the CO_2^* contributions in bandpass filtered measurements have little influence.

6.2 Axial Distributions. Figure 10 shows the axial distribution of the chemiluminescence intensities and the heat release rate for the $\lambda = 1.2$ operation point. The characteristics of the distributions and the conclusions drawn for this operation point are the same for all operation points investigated in this study.

The influence of the CO_2^* contribution in the bandpass filtered signals can be seen clearly from the normalized chemiluminescence distributions: Close to the burner exit ($x/D < 0.5$) and at axial distances $x/D > 3.0$ the CO_2^* contribution strongly distorts the shape of the radical intensities in the bandpass filtered measurements. The relative CO_2^* contribution in the bandpass filtered signals at axial distances $x/D < 0.5$ and $x/D > 3.0$ is higher than at axial distances between $0.5 < x/D < 3.0$. Close to the burner exit and at high axial distances almost the complete bandpass filtered signals consists of CO_2^* chemiluminescence. As a consequence, substantial errors are done when bandpass filtered chemiluminescence signals are interpreted as radical intensities. The CO_2^* contribution corrected CH^* signal is the best approximation of the heat release distribution, even though a significant downstream shift remains.

This obvious downstream shift of the chemiluminescence signals compared with the heat release is the second observation in Fig. 10. Since the air excess ratio is almost constant near the burner exit (Fig. 3) this effect is not caused by the ambient air entrainment. The shift can be explained with the local turbulence intensities in the flame. For the flames under investigation in this study the turbulence intensity in the reaction zone is high near the burner exit ($x/D < 1$). With increasing axial distance from the burner exit the turbulence intensity in the reaction zone decreases. Figure 11 shows on the left hand side the reaction progress of combustion as an indicator for the reaction zone, and on the right hand side the local turbulence intensity. The contours indicate a reaction progress of 0.1, 0.5, and 0.9, and represent the time averaged reaction zone of the flame. For $x/D < 1$, the three contours are close together in a region of high turbulence intensity. Further downstream the reaction zone becomes wider with a lower turbu-

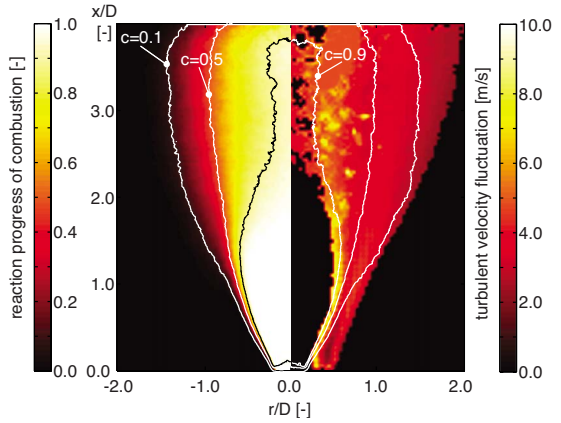

Fig. 11 Comparison of reaction progress of combustion (left hand side) and turbulence intensity (right hand side). The contours indicate the time averaged reaction zone with a reaction progress of 0.1, 0.5, and 0.9.

lence intensity. The observed downstream shift is due to quenching of the chemiluminescence in the region close to the burner exit and is similar to the effect reported by John and Summerfield [11], Hurle et al. [12], and Ayoola et al. [18].

The findings in this section are identical for all investigated operating points in this study. Thus, it can be concluded that the observed shift between heat release distribution and chemiluminescence distribution is independent of the air excess ratio and the integral heat release rate of the flame, respectively. This indicates that a similar shift is also to be expected in confined, adiabatic flames without mixture gradients.

6.3 Flame Length. In many applications a characteristic value of the chemiluminescence distribution is used as the measure for flame length. One characteristic value, which is commonly used, is the location of the maximum emission x_{max}. Figure 12 shows the burner air excess ratio dependency of x_{max} for the heat release rate and chemiluminescent emissions. Because of the quenched chemiluminescence near the burner exit the flame appears to be longer than indicated by the maximum heat release rate. It can be observed that the CO_2^* contributions in the bandpass filtered measurements have little effect on locations of maximum emission.

Similar results were observed for other definitions for the flame length, such as the balance point of the axial distributions. As pointed out before, similar discrepancies between a chemiluminescence based flame length and the actual flame length are also to be expected for confined, adiabatic flames without mixture gradients. This means that for turbulent swirl stabilized flames no reliable information about flame length can be obtained from chemiluminescence measurements.

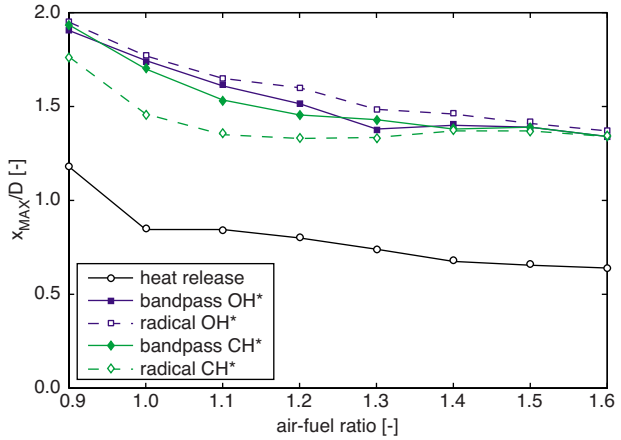

Fig. 12 Comparison of the location of maximum emission

7 Conclusions

In this experimental study the applicability of chemiluminescence as the measure for heat release rate in turbulent, swirl stabilized flames with mixture gradients has been investigated. For reference, a heat release rate measurement technique has been used, which is based on the first law of thermodynamics. The results of this technique have been discussed and have been found to be in good agreement with theoretical expectations and former publications.

The determined heat release rate has been compared with traditionally bandpass filtered chemiluminescence in the wavelength range of OH^* and CH^*, and with the integral chemiluminescence from the CO_2^* contribution corrected radical emissions. It has been found that the integral heat release of the flame and the integral chemiluminescence emission of any of the investigated species show an identical monotonic behavior. However, the axial heat release distribution is not properly represented by any signal either from OH^* or CH^*. The reason for this has been found in the high turbulence intensity in the reaction zone close to the burner exit. In this region of the flame the chemiluminescence is quenched, which results in a downstream shift of the chemiluminescence distribution compared with the actual heat release rate distribution. As a consequence, the flame appears to be longer than it is in reality. This observation is not limited to the flames investigated in this study. Similar effects have to be expected for all turbulent, swirl stabilized flames.

It can be concluded that chemiluminescence can be used to monitor the integral heat release of turbulent flames, if an empiric correlation between chemiluminescence and heat release can be obtained, which implies a known integral heat release of the flame. This is especially important for the use of chemiluminescence for the investigation of dynamic phenomena, such as the measurement of flame transfer functions. But no reliable information about the spatially resolved heat release rate distribution can be obtained from chemiluminescence data for turbulent, swirl stabilized flame.

Acknowledgment

The authors gratefully acknowledge the financial support provided by the DFG through the research unit "Chemilumineszenz und Wärmefreisetzung."

Nomenclature

Re = Reynolds number
$\dot{q}$ = volumetric heat release (W/m^3)
T = temperature (K)
c_p = isobaric heat capacity (kJ/kg K)
ρ = density (kg/m^3)
c = time averaged reaction progress of combustion
λ = air excess ratio
$\vec{v}$ = velocity (m/s)
C = proportionality constant
F = self-similarity function
T_ν = transmission
I = intensity
S = measurement signal
D = burner nozzle diameter (mm)
d = burner center body diameter (mm)
λ_ν = wavelength (nm)
x = axial coordinate
r = radial coordinate
* = chemiluminescent
BP = bandpass

References

[1] Auer, M., Gebauer, C., Mösl, K., Hirsch, C., and Sattelmayer, T., 2005, "Active Instability Control: Feedback of Combustion Instabilities on the Injection of Gaseous Fuel," ASME J. Eng. Gas Turbines Power, **127**, pp. 748–754.

[2] Auer, M., Hirsch, C., and Sattelmayer, T., 2005, "Influence of the Interaction of Equivalence Ratio and Mass Flow Fluctuations on Flame Dynamics," *Proceedings of the ASME Turbo Expo*, Reno-Tahoe, NV.

[3] Freitag, E., Konle, H., Lauer, M., Hirsch, C., and Sattelmayer, T., 2006, "Pressure Influence on the Flame Transfer Function of a Premixed Swirling Flame," *Proceedings of the ASME Turbo Expo*, Barcelona, Spain.

[4] Konle, M., Kiesewetter, F., and Sattelmayer, T., 2008, "Simultaneous High Repetition Rate PIV-LIF-Measurements of CIVB Driven Flashback," Exp. Fluids, **44**, pp. 529–538.

[5] Wäsle, J., Winkler, A., and Sattelmayer, T., 2005, "Spatial Coherence of the Heat Release Fluctuations in Turbulent Jet and Swirl Flames," Flow, Turbul. Combust., **75**, pp. 29–50.

[6] Wäsle, J., Winkler, A., Lauer, M., and Sattelmayer, T., 2007, "Combustion Noise Modeling on Experimental Data Using Chemiluminescence as an Indicator for Heat Release Distribution," *Proceedings of the European Combustion Meeting*.

[7] Wäsle, J., 2007, "Vorhersage der Lärmemission turbulenter Vormischflammen," Ph.D. thesis, TU München, Germany.

[8] Winkler, A., 2007, "Validierung eines Modells zur Vorhersage turbulenten Verbrenungslärms," Ph.D. thesis, TU München, Germany.

[9] Balachandran, R., Ayoola, B. O., Kaminski, C. F., Dowling, A. P., and Mastorakos, E., 2005, "Experimental Investigation of the Nonlinear Response of Turbulent Premixed Flames to Imposed Inlet Velocity Oscillations," Combust. Flame, **143**, pp. 37–55.

[10] Clark, T., and Bittker, D., 1954, "A Study of the Radiation From Laminar and Turbulent Open Propane-Air Flames as a Function of Flame Area, Equivalence Ratio, and Fuel Flow Rate," NACA Report No. RM E54F29.

[11] John, R., and Summerfield, M., 1957, "Effect of Turbulence on Radiation Intensity From Propane-Air Flames," Jet Propul., **27**, pp. 169–179.

[12] Hurle, I. R., Price, R. B., Sugden, T. M., and Thomas, A., 1968, "Sound Emission From Open Turbulent Premixed Flames," Proc. R. Soc. London, Ser. A, **303**, pp. 409–427.

[13] Samaniego, J.-M., Egolfopoulos, F., and Bowman, C., 1995, "CO_2^* Chemiluminescence in Premixed Flames," Combust. Sci. Technol., **109**, pp. 183–203.

[14] Haber, L., Vandsburger, U., Saunders, W., and Khanna, V., 2000, "An Experimental Examination of the Relationship Between Chemiluminescent Light Emissions and Heat-Release Rate Under Non-Adiabatic Conditions," *RTO AVT Symposium on Active Control Technology for Enhanced Performance Operational Capabilities of Military Aircraft, Land Vehicles and Sea Vehicles*, Braunschweig, Germany, 8–11 May, published in RTO MP-051.

[15] Lee, J., and Santavicca, D., 2003, "Experimental Diagnostics for the Study of Combustion Instabilities in Lean Premixed Combustors," J. Propul. Power, **19**(5), pp. 735–750.

[16] Najm, H., Paul, P., Mueller, C., and Wyckoff, P., 1998, "On the Adequacy of Certain Experimental Observables as Measurements of Flame Burning Rate," Combust. Flame, **113**, pp. 312–332.

[17] Fanaca, D., Alemela, P., Ettner, F., Hirsch, C., Sattelmayer, T., and Schuermans, B., 2008, "Determination and Comparison of the Dynamic Characteristics of a Perfectly Premixed Flame in Both Single and Annular Combustion Chambers," *Proceedings of the ASME Turbo Expo*, Berlin, Germany.

[18] Ayoola, B., Balachandran, R., Frank, J., Mastorakos, E., and Kaminski, C., 2006, "Spatially Resolved Heat Release Rate Measurements in Turbulent Premixed Flames," Combust. Flame, **144**, pp. 1–16.

[19] Wäsle, J., Winkler, A., Rössle, E., and Sattelmayer, T., 2006, "Development of an Annular Porous Burner for the Investigation of Adiabatic Unconfined Flames," *Proceedings of the 13th International Symposium on the Application of Laser Techniques to Fluid Mechanics*.

[20] Lauer, M., and Sattelmayer, T., 2007, "Luftzahlmessung in einer turbulenten Drallflamme auf Basis spektral aufgelöster Chemilumineszenz," VDI-Ber., **1988**, pp. 735–741.

[21] Lauer, M., and Sattelmayer, T., 2008, "Heat Release Calculation in a Turbulent Swirl Flame From Laser and Chemiluminescence Measurements," *Proceedings of the 14th International Symposium on Applications of Laser Techniques to Fluid Mechanics*.

[22] Haber, L., 2000, "An Investigation Into the Origin, Measurement and Application of Chemiluminescent Light Emissions From Premixed Flames," MS thesis, Virginia Polytechnic Institute and State University, Blacksburg, VA.

[23] Hardalupas, Y., and Orain, M., 2004, "Local Measurements of the Time-Dependent Heat Release Rate and Equivalence Ratio Using Chemiluminescent Emission From a Flame," Combust. Flame, **139**, pp. 188–207.

[24] Ikeda, Y., Nishiyama, A., Kim, S. M., Kawahara, N., and Tomita, E., 2006, "Anchor Point Structure Measurements for Laminar Propane/Air and Methane/Air Premixed Flames Using Local Chemiluminescence Spectra," *Proceedings of the 31st International Symposium on Combustion*.

[25] Nori, V., and Seitzman, J., 2007, "Chemiluminescence Measurements and Modeling in Syngas, Methane and Jet-A Fueled Combustors," *Proceedings of the AIAA*.

[26] Hoffmann, A., 2004, "Modellierung turbulenter Vormischverbrennung," Ph.D. thesis, Universität Karlsruhe (TH), Germany.

[27] Dribinski, V., Ossadtchi, A., Mandelshtam, V. A., and Reisler, H., 2002, "Reconstruction of Abel-Transformable Images: The Gaussian Basis-Set Expansion Abel Transform Method," Rev. Sci. Instrum., **73**, pp. 2634–2642.

[28] Eckbreth, A. C., 1996, *Laser Diagnostics for Combustion Temperature and Species*, 2nd ed., W. A. Sirignano, ed., Gordon and Breach, The Netherlands.